

Gibbs Monolayers at the Air/Water Interface: Surface Partitioning and Lateral Mobility of an Electrochemically Active Surfactant

Andrew D. Malec, Deng Guo Wu, Mary Louie, Janusz J. Skolimowski,[†] and Marcin Majda*

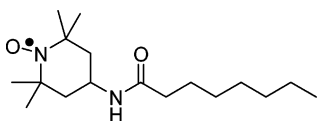
Department of Chemistry, University of California, Berkeley, Berkeley, California 94720-1460

Received September 18, 2003. In Final Form: November 13, 2003

Monolayer films of a water-soluble surfactant, 4-octaneamido-2,2,6,6-tetramethyl-1-piperidinyloxy (C₈-TEMPO) were investigated at the air/water interface. An electrochemical, horizontal touch method was developed to measure the equilibrium surface concentrations (Γ) of C₈TEMPO. The dependence of Γ on the solution concentration followed a Langmuir isotherm and yielded the partition constant $K = (2.3 \pm 0.2) \times 10^4 \text{ M}^{-1}$. These results were verified by surface tension measurements and Brewster angle microscopy. Within experimental error, the same K values were obtained. The lateral diffusion constants vs surface concentration of this molecule were measured by 2D voltammetry. In these experiments, the component of the oxidation current due to C₈TEMPO in the bulk of the solution was subtracted from the total measured current to obtain the component due to the lateral surface diffusion. In the range of mean molecular areas from 120 to 400 Å²/molecule, the lateral diffusion constant of C₈TEMPO increased from 1.0×10^{-6} to $1.0 \times 10^{-5} \text{ cm}^2/\text{s}$. The latter value is about 2.5 times larger than the C₈TEMPO diffusion constant in bulk water. Comparison of the lateral mobilities of C₈TEMPO and two longer alkane chain, water-insoluble homologues, C₁₄TEMPO and C₁₈TEMPO, showed no statistically significant differences.

Introduction

Surface equilibria and dynamics of water-soluble surfactants constitute fundamental elements of characterization of this important class of chemical systems.^{1,2} Specifically, understanding the bulk/surface partitioning, its dynamics, and the lateral surface mobility of water-soluble surfactants is essential to characterization of practical systems such as emulsions and foams. Understanding of these processes reflects also on our understanding of the properties of the aqueous liquid/vapor interfacial region, a subject of both fundamental significance and far-reaching significance in areas such as atmospheric sciences.^{3–5}



Here, we focus on redox-active, water-soluble surfactants represented in this study by an octane derivative of 4-amino-2,2,6,6-tetramethyl-1-piperidinyloxy (C₈TEMPO).

Taking advantage of the reversible and kinetically facile electroactivity of the nitroxide group,^{6,7}

$>\text{N}-\text{O}-\text{e}^- \rightleftharpoons >\text{N}=\text{O}^+$, we developed electrochemical methods to measure the equilibrium surface concentration of this surfactant at the air/water interface, as well as its lateral mobility on the water surface as a function of its bulk concentration. To measure the surface concentration of C₈TEMPO at the air/water interface, we broaden the horizontal touch methodology of Lipkowski and Bizzotto and co-workers.^{8–10} We used two time-resolved electrochemical techniques, cyclic voltammetry and chronocoulometry, to discriminate against electrochemical signal due to the C₈TEMPO bulk population. In the second part of these investigations, the lateral diffusion constant of C₈TEMPO is measured by 2D voltammetry.¹¹ In those experiments, we take advantage of differences in the diffusion-limited processes governing transport to a microelectrode of the two C₈TEMPO populations, that in the bulk of water and that at the air/water interface. We demonstrate that the signal due to the former can be independently recorded after the water surface is blocked by a compact monolayer of stearic acid, a redox-inactive and water-insoluble surfactant. When the resulting current–voltage curve is subtracted from that obtained in the absence of stearic acid, the differential signal can be interpreted to yield the lateral diffusion constant. The dependence of the lateral mobility of C₈TEMPO on its surface concentration is compared to the surface mobility data of longer chain length, water-insoluble derivatives of this surfactant, C₁₄TEMPO, and C₁₈TEMPO.¹²

* Corresponding author: e-mail majda@socrates.berkeley.edu, fax (510) 642-0269.

[†] Permanent address: Department of Organic Chemistry, University of Lodz, ul. Narutowicza 68, 90-136 Lodz, Poland.

(1) Dukhin, S. S.; Kretschmar, G.; Miller, R. *Dynamics of Adsorption at Liquid Interfaces. Theory, Experiment, Application*; Elsevier: Amsterdam, 1995.

(2) Fainerman, V. B.; Miller, R.; Moehwald, H. *J. Phys. Chem. B* **2002**, *106*, 809–819.

(3) Richmond, G. L. *Chem. Rev.* **2002**, *102*, 2693–2724.

(4) Pratt, L. R.; Pohorille, A. *Chem. Rev.* **2002**, *102*, 2671–2692.

(5) Lipowsky, R.; Sackman, E. *Structure and Dynamics of Membranes*; Elsevier: Amsterdam, 1995.

(6) Krzyczmonik, P. H. S. *J. Electroanal. Chem.* **1992**, *335*, 233–251.

(7) Baur, J. E.; Wang, S.; Brandt, M. C. *Anal. Chem.* **1996**, *68*, 3815–3821.

(8) Noel, J. J.; Bizzotto, D.; Lipkowski, J. *J. Electroanal. Chem.* **1993**, *344*, 343–354.

(9) Bizzotto, D.; Noel, J. J.; Lipkowski, J. *Thin Solid Films* **1994**, *248*, 69–77.

(10) Bizzotto, D.; Noel, J. J.; Lipkowski, J. *J. Electroanal. Chem.* **1994**, *369*, 259–265.

(11) Majda, M. in *Thin Films*, Vol. 20, *Organic Thin Films and Surfaces. Directions for the Nineties*; Ulman, A., Ed.; Academic Press: New York, 1995; pp 331–347.

(12) Johnson, M. J.; Anvar, D. J.; Skolimowski, J. J.; Majda, M. *J. Phys. Chem. B* **2001**, *105*, 514–519.

Experimental Section

Materials. Synthesis of 4-octaneamido-2,2,6,6-tetramethyl-1-piperidinyloxy free radical (C_8 TEMPO) followed the same procedure as that used in the synthesis of the octadecane derivative (C_{18} TEMPO) described earlier.¹³ Briefly, octanoyl chloride was reacted with 4-amino-TEMPO in methylene chloride and the resulting carboxamide was oxidized with hydrogen peroxide in the presence of sodium tungstate/ethylenediamine-tetraacetic acid (EDTA) catalyst in a solution of 1:6 acetone/water. Purification of the product was performed by column chromatography (silica gel, eluted with 35% ethyl acetate in hexane) and characterized by thin-layer chromatography (TLC) and elemental analysis. The product crystallized slowly after vacuum evaporation. The crystals were then incubated in a vacuum to remove any traces of solvent remaining. The final results of the elemental analysis experiments were (calcd) C 68.6, H 11.2, N 9.4; (found) C 68.3, H 11.5, N 9.1. The melting point was 40 °C.

Octadecyltrichlorosilane (OTS) and 3-mercaptopropyltrimethoxysilane (MPS) were from Aldrich. OTS was vacuum-distilled into sealed glass ampules, which were opened as needed immediately prior to the individual experiments. Octadecylmercaptan (OM) (Tokyo Kadei, Tokyo, Japan) was used without further purification. Reagent-grade 70% $HClO_4$ (Fisher, ACS-certified), $LiClO_4$ (99.99%, Aldrich), *n*-alkanethiols (C_nSH , $n = 3, 6, 9, \text{ and } 12$; Aldrich), ACS-certified spectra analyzed chloroform, and all other chemicals were used as received without further purification. House-distilled H_2O was passed through a four-cartridge Millipore purification train, and a 0.2 μm hollow-fiber final filter. The resistivity of the resulting water (DI water) was 18.3 M Ω cm.

Line Electrode Fabrication. Two-dimensional electrochemical measurements at the air/water interface required specially designed "line" microelectrodes that are placed to touch the water surface and which self-position to become aligned exactly with the plane of the air/water interface.^{11–13} They were produced by creating a sharp gradient of wettability along a fracture line of ~ 80 nm thick gold films, vapor-deposited on microscope glass slides (ca. 8×20 mm²). The pattern of the deposited gold film includes two circular areas and a strip of gold (0.5 mm in width) connecting them. The circular areas were later used as electrical contacts while the edge of the strip becomes the line electrode after the slide was fractured by scribing it with a diamond pencil. The fabrication of these electrodes was previously described in detail.¹³

Horizontal Touch Experiments. Experiments at the air/water interface were performed in a custom-made round Teflon trough (diameter ~ 5 cm, depth ~ 1 cm). Single-crystal gold electrodes used in the horizontal touch experiments were cut to expose a surface of random crystallographic orientation of ca. 0.25 cm². The electrode was polished flat while embedded in an aluminum holder with an epoxy resin, by use of first sandpaper of increasing grit (to 600) and then a series of alumina and silica polishing compounds from 5 to 1 to 0.3 and finally 0.05 μm particles. The electrode was then removed from the mold, and a short piece of gold wire connected to a longer piece of heavy copper wire was welded to the crystal to allow easy handling and to serve as electrical connection. In all subsequent experiments, the gold electrode was used in the horizontal touch mode, positioned just above the water surface with the polished surface supporting a slightly positive meniscus of water beneath it. The exact surface area of the polished surface was measured by comparing the voltammetric peak currents recorded in a 1 mM $Ru(NH_3)_6Cl_3$ and 0.1 M KCl solution by use of the single-crystal gold electrode and a hanging Hg drop electrode of precisely known surface area. In the experiments involving the measurements of the C_8 TEMPO surface concentration, the flat surface of the gold was modified with a monolayer of an alkanethiol (C_nSH , $n = 3, 6, 9, \text{ or } 12$). This was accomplished by placing a drop of ~ 0.5 mM *n*-alkanethiol ethanol solution on the electrode surface. The drop was allowed to rest on the surface for ~ 10 s and then it was rinsed with copious amounts of ethanol and dried with N_2 . For $C_{12}SH$ coating, the solvent was 2-propanol rather than ethanol.

Following each set of horizontal touch experiments, the gold surface was brought back to its initial state by several careful flaming cycles that increased the temperature of the gold crystal to just below melting point, visually recognized by a dark red color of the crystal followed by quenching in distilled water.

Electrochemical Measurements. All cyclic voltammetric and chronocoulometric experiments were done with either a CH Instruments Model 620 electrochemical analyzer (Austin, TX) or a BAS Model 100A electrochemical analyzer (West Lafayette, IN) in a three-electrode setup under computer control with an SCE or a Ag quasi-reference electrode and a Pt counterelectrode. A copper Faraday cage was used in 2D electrochemical experiments to minimize noise.

Brewster Angle Microscopy. Brewster angle microscopy (BAM) measurements were performed on a small active vibrational table (MOD-2, Halcyonics GmbH, Goettingen, Germany) enclosed in a Plexiglas box on a large table within a thermostated, laminar flow enclosure operated under positive pressure with filtered air. The microscope (BAM2plus, Nanofilm Technologie GmbH, Goettingen, Germany) was equipped with a 50 mW Nd:YAG laser, typically operated at 50% power. BAM measurements were done in ca. 10 s exposures interspersed by ca. 30 s for a total time of about 5–10 min at each concentration.

Surface Tension Measurements. Surface tension measurements of the C_8 TEMPO solutions were done with a DuNouy tensiometer (model 70535, CSC Scientific Co. Inc.). The tensiometer's Pt ring was flamed between each measurement to increase the precision and reproducibility of these measurements.

Results and Discussion

Determination of Surface Concentration. The horizontal touch method of Lipkowski and Bizzotto is applicable to our system.^{8–10} Briefly, a flat surface of an unmounted gold single crystal (see Experimental Section) is brought into contact with the water surface and positioned slightly above the surface supporting a positive meniscus of water and thus limiting the exposed surface area of the gold crystal to its flat surface. In our case, featuring a solution of a water-soluble TEMPO surfactant, the gold surface is then contacting the C_8 TEMPO monolayer. Since surface adsorption of a surfactant is driven by a decrease of the interfacial tension, the surface concentration of C_8 TEMPO at the solution/gold interface can be expected to be different than the equilibrium concentration of C_8 TEMPO at the air/water interface since the interfacial tension of the two interfaces is different. Therefore, our first goal was to chemically modify the gold surface by assembling a monolayer of an alkanethiol so that the energetics of the modified gold/water interface approximate the energetics of the alkane/water interface. Specifically, at 20 °C, the surface tensions of the air/water and alkane/water interfaces are 72.4 and 51.4 ± 0.5 mN/m (the latter is the average and the standard deviation of the nearly identical interfacial tensions of water and six liquid hydrocarbons of increasing chain length from hexane to dodecane).¹⁴ The interfacial tension of an alkanethiol-modified gold/water interface is likely to be somewhat smaller than that of the alkane/water interface. Consequently, in view of the thermodynamic argument mentioned above, we could expect a small negative error in the C_8 TEMPO surface concentrations determined at the modified gold/water interface relative to the air/water interface. We discuss this issue below.

In addition to surface thermodynamics, we were also concerned about the effect of the alkanethiol monolayer on the electron-transfer processes involved in the C_8 -TEMPO coulometric assay. As described in the Experimental Section, the assembly of C_nSH ($n = 3, 6, 9, \text{ and } 12$)

(13) Johnson, M. J.; Majmudar, C.; Skolimowski, J. J.; Majda, M. J. *Phys. Chem. B* **2001**, *105*, 9002–9010.

(14) Dukhin, S. S.; Kretzschmar, G.; Miller, R. *Dynamics of Adsorption at Liquid Interfaces. Theory, Experiment, Application*, Elsevier: Amsterdam, 1995; p. 530.

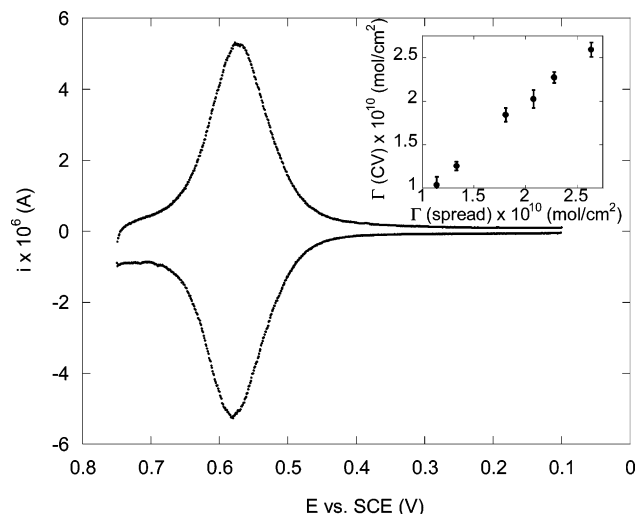


Figure 1. Cyclic voltammogram of C_{18} TEMPO recorded at $75 \text{ \AA}^2/\text{molecule}$ on the surface of a 50 mM LiClO_4 and 10 mM HClO_4 solution; $\nu = 0.05 \text{ V/s}$. (Inset) Correlation plot of the C_{18} TEMPO surface concentrations measured by the horizontal touch voltammetry and that spread on the water surface from a C_{18} -TEMPO chloroform solution.

was limited to 10 s in order to decrease the extent of organization and thus potentially passivating character of the monolayer films. The resulting water contact angles measured on the modified gold surfaces were 92° , 96° , 99° , and 101° , respectively. We further determined that the surface concentrations of C_8 TEMPO measured with C_{12} SH-modified gold electrodes were systematically ca. 14% lower than those obtained when a nonanethiol modification layer was used. We assigned this difference to partial blocking of the C_8 TEMPO electroactivity by the dodecanethiol monolayer. The C_8 TEMPO coverage obtained with nonanethiol-modified electrodes was ca. 3% and 22% greater than those obtained with the C_6 SH- and C_3 SH-modified surfaces, respectively. Consequently, all the data shown below were obtained with either the hexanethiol- or the nonanethiol-modified gold ($C_{6,9}$ S-Au) electrodes.

Initially, we tested the $C_{6,9}$ S-Au electrodes in the horizontal touch experiments involving water-insoluble monolayers of C_{18} TEMPO.¹³ Figure 1 shows a cyclic voltammogram recorded in such experiments with the C_{18} TEMPO surface coverage of $2.2 \times 10^{-10} \text{ mol/cm}^2$ (corresponding to $75 \text{ \AA}^2/\text{molecule}$). Integration of the anodic or cathodic current above background yields the electrochemically determined surface coverage. The inset in Figure 1 is a correlation of the electrochemically determined coverage and that spread on the water surface by a standard Langmuir trough procedure with a chloroform solution of C_{18} TEMPO of a precisely known concentration.¹³ The unit slope in that correlation in a range of the surface concentrations of $(1.1\text{--}2.6) \times 10^{-10} \text{ mol/cm}^2$ ensure us that the $C_{6,9}$ S-Au electrodes allow full electroactivity of C_{18} TEMPO trapped at the $C_{6,9}$ S-Au/water interface.

Determination of the C_8 TEMPO surface concentration is only slightly more involved. Since the surface population of C_8 TEMPO is in equilibrium with its bulk population, the horizontal touch cyclic voltammograms reveal current contributions of both populations. The two components of the voltammetric current can be resolved by one of two methods. The first is voltammetry at a fast scan rate (ν) such that the diffusion-controlled current due to oxidation of the bulk population ($i_b \propto \nu^{1/2}$) is insignificant relative to the surface current proportional to the C_8 TEMPO

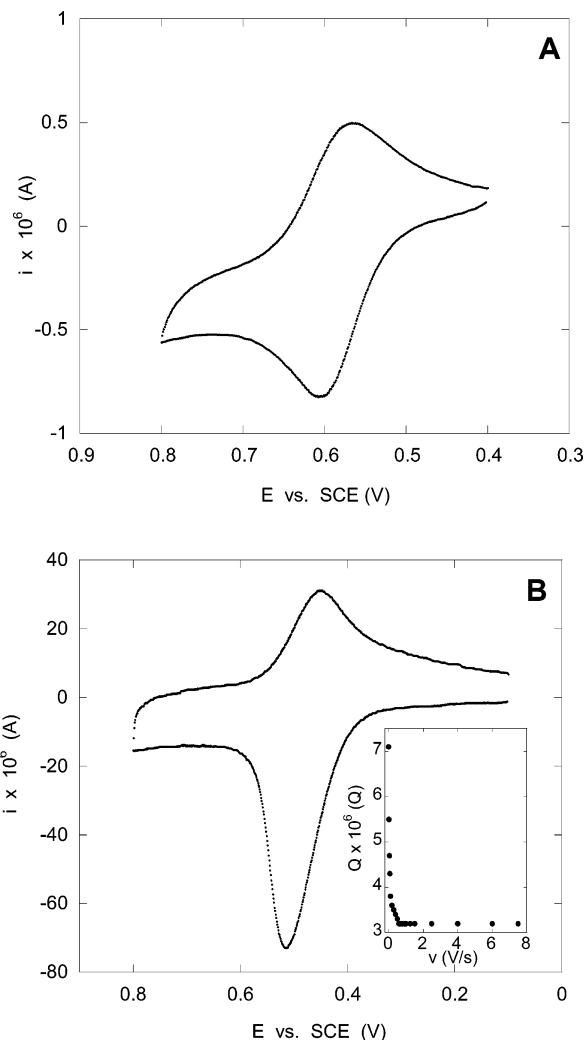


Figure 2. Horizontal touch cyclic voltammograms of a $4.47 \times 10^{-5} \text{ M}$ solution of C_8 TEMPO in 50 mM LiClO_4 and 10 mM HClO_4 electrolyte recorded with a C_6 S-Au electrode at a scan rate of 0.01 V/s (A) and 2.0 V/s (B). (B, inset) Plot of charge due to oxidation of C_8 TEMPO obtained by integrating the anodic peak current vs scan rate.

concentration at the $C_{6,9}$ S-Au/water interface ($i_s \propto \nu$).¹⁵ Figure 2 shows two cyclic voltammograms of C_8 TEMPO at a bulk concentration of $4.47 \times 10^{-5} \text{ M}$ recorded in the horizontal touch experiments at 0.01 and 2 V/s. The slow-scan voltammogram (Figure 2A) is dominated by the C_8 -TEMPO bulk component. As a result, its anodic and cathodic branches are of nearly identical magnitude. The symmetric shape of the anodic peak of the fast-scan voltammogram (Figure 2B) reveals the dominance of the C_8 TEMPO surface component. The asymmetry of the anodic and cathodic branches in this case reflects a greater solubility of the positively charged oxonium ion, C_8 -TEMPO⁺ a fraction of which leaves the $C_{6,9}$ S-Au/water interface before it can be reduced. Integration of the anodic current of the high-scan voltammograms yields the surface concentration of C_8 TEMPO. Analysis of the dependence of the surface concentration obtained in such experiments on scan rate (see inset in Figure 2B) showed that the anodic charge became independent of scan rate above ca. 1 V/s. Thus, at scan rates higher than 1 V/s, the contribution to the anodic current due to the bulk population of C_8 TEMPO becomes insignificant.

(15) Bard, A. J.; Faulkner, L. R. *Electrochemical Methods. Fundamentals and Applications*, 2nd ed.; J. Wiley & Sons: New York, 2001.

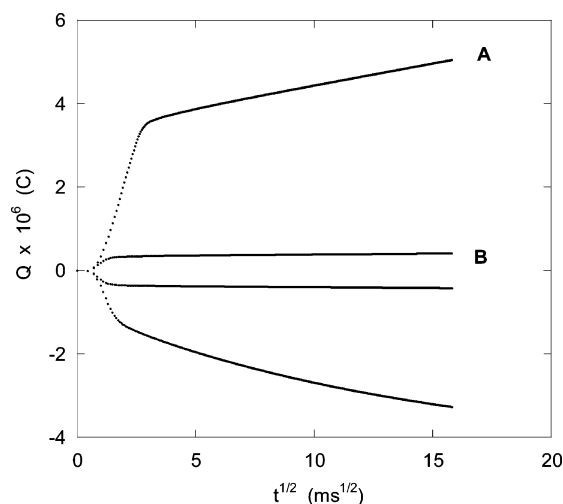


Figure 3. Anson plots (Q vs $t^{1/2}$) corresponding to the chronocoulometric experiments involving a $C_{6,9}S$ -Au electrode touching a 4.47×10^{-5} M C_8 TEMPO, 50 mM $LiClO_4$, and 10 mM $HClO_4$ solution. A 300 ms potential step was applied from 0.250 to 0.550 V (A) and from -0.050 to 0.250 mV (B) vs SCE.

Chronocoulometry is the other time-resolved method that allows us to determine the surface population of C_8 -TEMPO in the presence of its bulk component.¹⁵ In this potential step experiment, the time dependence of charge (Q) is given by

$$Q = Q_{dl} + nFA\Gamma + 2nFAC^* \sqrt{\frac{D_b t}{\pi}} \quad (1)$$

where Q_{dl} is the double-layer charge associated with the potential change, Γ is the surface concentration of C_8 -TEMPO at the $C_{6,9}S$ -Au/water interface, D_b is the diffusion constant of C_8 TEMPO in water, and the other symbols carry their usual meanings. A plot of Q vs $t^{1/2}$ gives Γ from its intercept once the double-layer charge is independently determined. Figure 3 shows one such plot representing a chronocoulometric experiment carried out on a 4.47×10^{-5} M C_8 TEMPO, 0.05 M $LiClO_4$, and 0.01 M $HClO_4$ solution. To accurately measure the double-layer charge, similar experiments were carried out stepping the potential in a range negative of the formal potential of C_8 TEMPO where no faradaic current flows (see Figure 3, curve B). A blank voltammogram recorded between -0.05 and $+0.55$ V at 1 V/s at a modified gold electrode touching 0.05 M $LiClO_4$ and 0.01 M $HClO_4$ electrolyte solution showed that the capacitance (C_{dl}) of the $C_{6,9}S$ -Au/solution interfaces is independent of the potential in this range. Therefore, the intercepts of the Anson plots such as those in Figure 3B represent the accurate value of Q_{dl} . We note that C_{dl} that can be obtained as $Q_{dl}/\Delta V$ is affected both by the modifying alkanethiol monolayer and by the adsorption of C_8 TEMPO. For example, the average C_{dl} of the C_6S -Au/water interfaces was found to be $5.6 \pm 0.1 \mu F/cm^2$. It decreases to $4.7 \pm 0.1 \mu F/cm^2$ when the electrode is exposed to the same electrolyte also containing 4.47×10^{-5} M C_8 TEMPO. The C_8 TEMPO surface concentration (Γ) data obtained by the fast-scan voltammetry and by chronocoulometry were statistically indistinguishable. We point out that surface coverage measured by these techniques does not depend on the time of equilibration of the C_6S -Au electrodes at the surface of the C_8 TEMPO solutions from approximately 1 s to over an hour. Figure 4 shows the dependence of Γ_{C_8TEMPO} on C_8 TEMPO bulk concentration obtained by these electrochemical methods.

To validate our new electrochemical methodology, the dependence of the surface concentration of C_8 TEMPO on

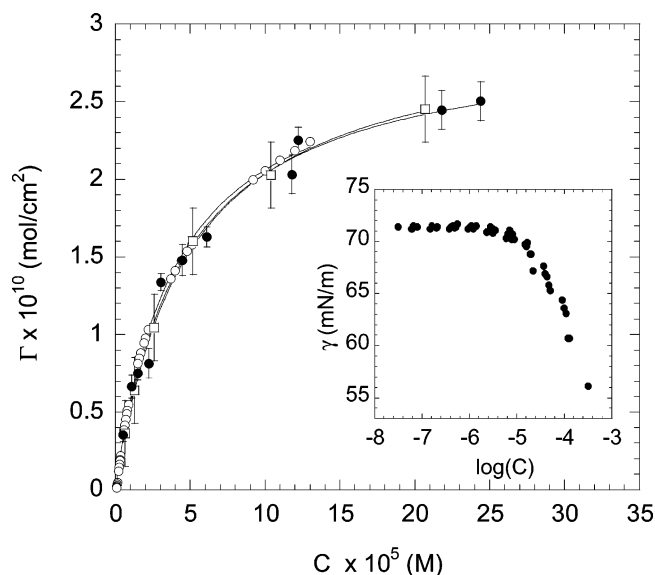


Figure 4. C_8 TEMPO surface vs solution concentration plots obtained by horizontal touch voltammetry (\bullet), surface tensiometry (\circ), and BAM (\square). The solid lines represent fits of the three sets of data to the Langmuir isotherm. The fitting parameters are listed in Table 1. (Inset) Plot of surface tension vs $\log C$ (molar) used to generate the surface tensiometry isotherm in the main plot.

Table 1. Langmuir Isotherm Fitting Parameters to the Data in Figure 4

method	$K \times 10^{-4}$ (L/mol)	$\Gamma_{max} \times 10^{10}$ (mol/cm ²)
BAM	2.2 ± 0.1	3.0 ± 0.1
electrochemistry	2.3 ± 0.2	2.9 ± 0.1
surface tension	2.5 ± 0.1	2.9 ± 0.1

its bulk concentration was also deduced from the measurements of the integrated reflected light intensity in Brewster angle microscopy (BAM), carried out on the C_8 -TEMPO solutions of increasing bulk concentration, and from a set of surface tension (γ) measurements. We demonstrated earlier that the intensity of reflected BAM light integrated over the illuminated area of the air/water interface of $320 \times 430 \mu m^2$ is, indeed, proportional to the surface concentration of a surfactant at that interface.¹³ The surface tension measurements (shown in the inset of Figure 4) yielded the surface concentration of C_8 TEMPO by use of the Gibbs equation:

$$\Gamma = -\frac{1}{RT} \frac{d\gamma}{d \ln(C)} \quad (2)$$

Both sets of the Γ vs C data are also shown in Figure 4. The solid lines in that figure represent the fits of the Langmuir isotherm to the three sets of data:

$$\Gamma = \Gamma_{max} \frac{KC}{1 + KC} \quad (3)$$

where K is the partitioning constant and Γ_{max} is the limiting surface concentration. The values of these parameters for each fit are listed in Table 1. Examination of Figure 4 and Table 1 shows clearly that there is very good agreement between the results of the three experimental approaches.

The comparison of the BAM, surface tension, and electrochemical data in Figure 4 requires some discussion. Unlike the first two methods, the electrochemical approach is specific to C_8 TEMPO. However, it relies on the determination of C_8 TEMPO at the $C_{6,9}S$ -Au/water interface rather than at the air/water interface. As mentioned above,

the fact that the former is expected to exhibit a smaller interfacial tension and thus presents a weaker driving force for C_8 TEMPO adsorption suggests that the electrochemical results in Figure 4 could be burdened with a systematic negative error. In comparison, the BAM and surface tension measurements could, in principle, be burdened with a positive error. While we do not believe that impurities play a significant role in the measurements reported in Figure 4, BAM and surface tensiometry are not specific to C_8 TEMPO but report rather an integrated effect due to all surface-active compounds including, potentially, impurities. Therefore, the agreement between the three sets of adsorption data suggests that they all accurately reflect the adsorption thermodynamics. Consequently, there likely exists an additional driving force in the C_8 TEMPO adsorption at the $C_{6,9}S$ -Au/water interface that compensates for the somewhat lower interfacial tension of that interface relative to the air/water interface. We postulate that this additional effect is due to intercalation of C_8 TEMPO into the alkanethiol monolayer on gold. The latter is clearly not well organized (see the contact angle data above) because of the purposefully short self-assembly time and the relatively short alkane chain. Even a prolonged self-assembly of alkanethiols results in well-ordered monolayer films exhibiting contact angles with water of ca. 112° only when the chain length is at least 12 carbon atoms long.¹⁶ The decrease of C_{dl} of the $C_{6,9}S$ -Au/water interface in the presence of C_8 TEMPO reported above substantiates this hypothesis.

Determination of the Lateral Diffusion Constant. Determination of the lateral diffusion constant of C_8 TEMPO encounters a similar difficulty as that met in the measurements of the surface concentrations. Existence of two C_8 TEMPO populations, on the water surface and in bulk of the aqueous solution, inevitably leads to the fact that the measured current at a gold line microelectrode is a sum of two components contributed by the two C_8 TEMPO populations.

The methodology of 2D voltammetry with line microelectrodes has been described in our previous reports.^{11–13} Briefly, in these experiments, the microband electrode obtained by fracturing a gold-coated glass slide (see Experimental Section) is touching the water surface so that only the cross-section of the newly generated glass slide and the ca. 100 nm wide edge of the vapor-deposited gold film are exposed to the electrolyte solution. Thus, the voltammetric current recorded with these microband electrodes (see Figure 5, curve A) contains a lateral component due to the surface population and a component due to the C_8 TEMPO bulk population. The latter can be independently recorded when the water surface is covered by a monolayer of stearic acid, which blocks adsorption of C_8 TEMPO. A small volume of a chloroform solution of stearic acid is spread on the surface in the electrochemical cell. The amount of stearic acid applied was equivalent to a mean molecular area of $15 \text{ \AA}^2/\text{molecule}$, well in excess of the full monolayer coverage. By comparing voltammograms of 4-hydroxy-TEMPO, a compound that does not partition to the air/water interface, in the presence and in the absence of a stearic acid film, we verified that the presence of the film does not affect our ability to accurately record current due to the bulk component. Voltammogram B in Figure 5 was recorded in the presence of a stearic acid film on the water surface. Its sigmoidal shape is independent of scan rate and reflects purely radial (hemicylindrical) diffusion, which is expected in these

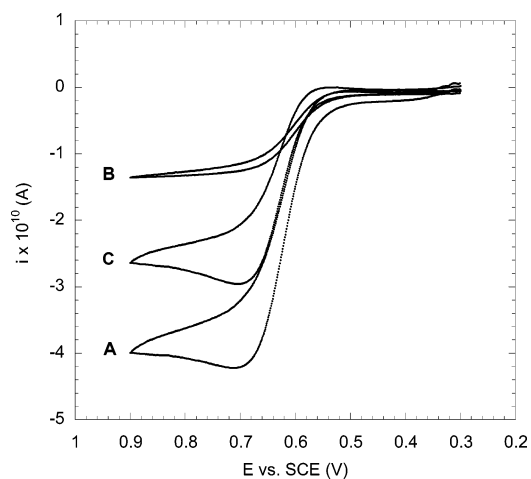


Figure 5. Two-dimensional cyclic voltammograms of C_8 -TEMPO recorded with a $590 \mu\text{m}$ line electrode on a $4.47 \times 10^{-5} \text{ M}$ C_8 TEMPO, 50 mM LiClO_4 , and 10 mM HClO_4 solution at $v = 5 \text{ mV/s}$ (curve A). Curve B was recorded under identical conditions after the solution surface was covered with a monolayer film of stearic acid. Curve C is the difference between traces A and B.

experiments in view of a very small, 100 nm width (w) of the microband electrodes. The plateau current at a fixed potential (and therefore time) can be interpreted to yield C_8 TEMPO bulk solution diffusion coefficient (D_b). We used a long time approximation of the ultramicroband chronoamperometric i vs t equation:¹⁵

$$i(t) = \frac{2\pi nFAD_b C^*}{w \ln(64D_b t/w^2)} \quad (4)$$

In a set of experiments carried out with stearic acid-covered water surface at different bulk C_8 TEMPO concentrations (C^* was varied in the range shown in Figure 4), the average D_b value and standard deviation were found to be $(3.9 \pm 0.24) \times 10^{-6} \text{ cm}^2/\text{s}$.

The ability to independently record the component of the voltammetric current due to the C_8 TEMPO diffusion in the bulk of electrolyte allows us then to subtract it from the current recorded in the absence of the stearic acid monolayer, and thus to obtain the 2D voltammogram due to the lateral diffusion of C_8 TEMPO on the water surface (see Figure 5, curve C). The cathodic branch of the voltammogram C in Figure 5 is very small due to the fact that the oxonium cation, $C_8\text{TEMPO}^+$, generated in the forward, anodic scan is more soluble in water than its reduced, uncharged counterpart and desorbs from the air/water interface. The anodic branch of the 2D voltammogram bears a signature of a mixed linear and radial diffusion. This is expected since the width of the diffusion layer developing in the plane of the water surface in these slow-scan experiments is comparable with the $590 \mu\text{m}$ length of our line microelectrodes. Therefore, the observed 2D voltammogram (curve C in Figure 5) combines a hemicylindrical and a linear diffusion component. To extract the lateral diffusion constant (D_s) of C_8 TEMPO, we relied on the equation derived by Aoki et al.¹⁷ for the case of linear sweep voltammetry at microcylinder electrodes that considers, as in our case, a mixed linear and hemicylindrical diffusion control of the peak current. The necessary 3D \rightarrow 2D reduction of dimensionality involved substituting the product of cylinder length (h) and bulk concentration

(16) Bain, C. D.; Troughton, E. B.; Tao, Y. T.; Evall, J.; Whitesides, G. M.; Nuzzo, R. G. *J. Am. Chem. Soc.* **1989**, *111*, 321–335.

(17) Aoki, K.; Honda, K.; Tokuda, K.; Matsuda, H. *J. Electroanal. Chem.* **1985**, *182* (2), 267–279.

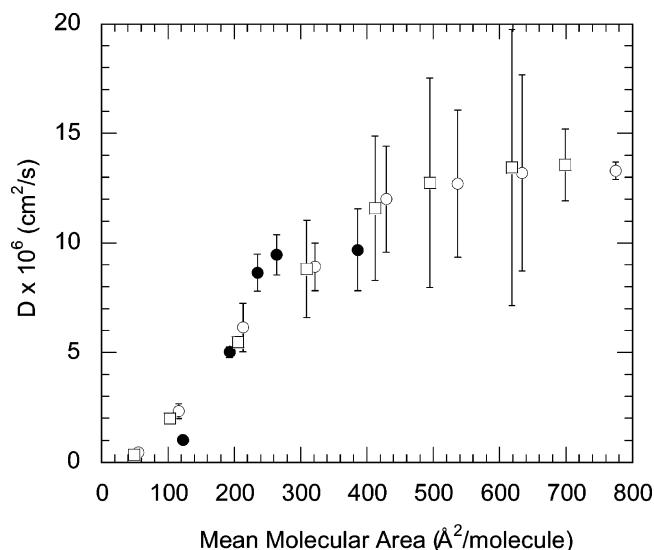


Figure 6. Plot of surface lateral diffusion constant vs mean molecular area of C₈TEMPO (●), C₁₄TEMPO (○), and C₁₈TEMPO (□).

(C) by surface concentration Γ , as described previously.¹⁸ We also relied on a well-established approximation stating that, in the limit of long times, current at a microband electrode with width w can be well approximated by current at a hemicylindrical electrode of radius r when one makes a substitution, $r = w/4$.¹⁹ These substitutions yielded the following (at 293 K):

$$i_p = (2.13 \times 10^5) \Gamma w D^{1/2} v^{1/2} + (1.09 \times 10^5) \Gamma w^{0.15} D^{0.925} v^{0.075} \quad (5)$$

We note that the width, w , is now represented by the length of our line microelectrode as explained earlier.¹⁸ The results are plotted in Figure 6, where the D_s values for the water-insoluble C₁₄TEMPO and C₁₈TEMPO obtained in similar experiments are also shown. It is interesting to note that the lateral diffusion of these three TEMPO derivatives with alkyl chains of substantially different length exhibits the same mobilities at the air/water interface. Clearly, their mobility is limited primarily by the viscous coupling of their polar fragments to water, their surface concentration, but not by the chain–chain interactions. The increase of the D values with mean molecular area of the surfactants in Figure 6 reflects the decreasing effective viscosity of the monolayer in the headgroup region as the concentration of the diffusing

particles decreases. This is consistent with the behavior of particle–fluid suspensions.^{20,21} A quantitative analysis of the data in Figure 6 will be a subject of a separate report. We note that in the case of the ferrocene-amide surfactants, which we investigated earlier, we did observe an alkane chain length effect on the surfactant mobility.²² However, in that case we showed that the effect was related to the dependence of the surfactant's immersion depth on the chain length and not directly to the chain–chain interactions. In closing, we note that the C₈TEMPO diffusion constant in low-density monolayers at the air/water interface of ca. 1.0×10^{-5} cm²/s is more than twice as large as its value in the bulk of the aqueous electrolyte of 3.9×10^{-6} cm²/s. This is the consequence of a rather shallow immersion depth of the TEMPO amphiphile at the air/water interface.

Conclusions

Our electrochemical, horizontal touch method of measuring surfactant's surface concentration at the air/water interface was compared with surface tension measurements and Brewster angle microscopy. The very good agreement of the data obtained by these three techniques suggests that surface modification of gold electrodes with either hexane- or nonanethiol generates, in contact with water, an interface that behaves similarly to the air/water interface, yielding the same partition constant for C₈TEMPO. We hypothesize that the smaller interfacial tension of that interface relative to that of the air/water interface is compensated by the van der Waals interactions of C₈TEMPO with the alkane chains of the alkanethiol monolayer. Whether this property of the C_{6–9}S-Au/water interface can be extended to other classes of redox-active surfactant is a subject of our current investigations. We also showed that line microelectrodes can be used successfully in the measurements of the lateral mobility of water-soluble redox surfactants at the air/water interface. Finally, we demonstrated that the lateral mobility of C_{*n*}TEMPO surfactants (with $n = 8, 14,$ and 18) does not depend on the length of their alkane chain. It is instead determined by their immersion depth and by their concentration, which determines the level of intermolecular interactions in the headgroup region.

Acknowledgment. We acknowledge the donors of the Petroleum Research Fund, administered by the American Chemical Society, for partial support of this research. Additional support was provided by the National Science Foundation (CHE-0079225).

LA035754G

(18) Charych, D. H.; Goss, C. A.; Majda, M. *J. Electroanal. Chem.* **1992**, *323*, 339–345.

(19) Szabo, A.; Cope, D. K.; Tallman, D. E.; Kovach, P. M.; Wightman, R. M. *J. Electroanal. Chem.* **1987**, *217*, 417–423.

(20) Ladd, A. J. C. *J. Chem. Phys.* **1990**, *93*, 3484–3494.

(21) Lionberger, R. A.; Russel, W. B. In *Advances in Chemical Physics*; Prigogine, I., Rice, S. A., Eds.; J. Wiley & Sons: New York, 2000; Vol. 111, pp 399–474.

(22) Kang, Y. S.; Majda, M. *J. Phys. Chem. B* **2000**, *104*, 2082–2089.